

LETTER TO THE JOURNAL

The interplay between natural killer cells and pancreatic stellate cells in pancreatic ductal adenocarcinoma

Pancreatic ductal adenocarcinoma (PDAC) remains one of medicine's most urgent areas of unmet need. With 5-year survival rates of ~11%, PDAC is set to become the second leading cause of cancer related deaths by 2040 [1]. The complex tumour microenvironment (TME) in PDAC, responsible for poor prognosis, is comprised of extracellular matrix (ECM) proteins and multiple cell types; with pancreatic stellate cells (PSCs), which become activated cancer associated fibroblasts (CAFs), being regarded as key orchestrators of the TME. We have demonstrated that treatment with all-trans retinoic acid (ATRA) can render activated PSCs (aPSC) to a quiescent (qPSC) phenotype (shift to G1 phase of cell cycle and other features [2]), resulting in stromal remodelling and thus, influencing cancer cell co-targeting with chemotherapy in patients [3]. This has resulted in the use of ATRA along with standard-of-care chemotherapy in the Stromal TARgeting for PANcreatic Cancer (STARPAC) clinical trial, with promising results [4]. These clinically relevant [5], exciting potential therapeutic benefits of stromal co-targeting through rendering PSCs quiescent [6], along with predictive inflammation-related biomarkers [7], and increased focus on cellular therapeutics such as NK cells, led us to postulate potential targetable PSC-immune cell interactions which may uncover a comprehensive therapeutic strategy for treating hitherto, incurable PDAC.

We identified differential NK-92 (a cell line representing NK cells) cytotoxicity against qPSCs (telomerase reverse transcriptase (hTERT) immortalised PS1 cell line rendered quiescent by administering ATRA for seven days at 1 $\mu\text{mol/L}$ daily [2]) and aPSC phenotypes as assessed by sur-

face expression of CD107a/b, and Calcein Acetyoxymethyl (AM) cytotoxicity assays (Supplementary Figure S1A-B). Furthermore, qPSC or aPSC education of NK-92 cells resulted in altered and distinct cytotoxicity towards pancreatic cancer cells (BxPC3, Capan2, MiaPaca2) as indicated by surface CD107a/b expression (Figure 1A) and complemented by Calcein AM cytotoxicity assays (data not shown).

Surface and intracellular markers for CAF subtypes (pCAF assigner subtypes A-D [3]; CD105^{+/-} CAFs [8]) and surface activating/inhibitory receptors and intracellular functional markers for NK cells, as assessed by spectral flow cytometry and Luminex ELISA secretome analysis, demonstrated that this interaction is, indeed, bidirectional. We demonstrated stellate cell polarisation to a myofibroblastic activation state [2] in response to direct contact with NK cells as assessed by alpha-SMA abundance (geometric mean fluorescence intensity (MFI)), as well as upregulation of CD105 expression, a CAF marker of anti-tumour immunity [8], irrespective of previous PSC activation status (Figure 1B), a fact not observed in Transwell™ separated co-culture (Supplementary Figure S1C) or conditioned media from NK cells (Supplementary Figure S1D), underlining the importance of direct cell-to-cell interaction.

Concomitantly, we observed an upregulation of TIM3 on NK cells in response to direct co-culture with both qPSC and aPSCs, but a differential increase in NKG2A expression in response to qPSC but not aPSC. Functional markers, such as Granzyme B and Perforin, were also found to be differentially expressed (Figure 1C) in direct co-culture but not in Transwell™ separated conditions (Supplementary Figure S1E). Secretome analysis of direct co-culture demonstrated clear upregulation of interferon- γ , C-X-C chemokine ligand (CXCL) 9, CXCL10, CXCL11, and other cytokines and chemokines, not observed in indirect co-culture conditions, explaining the obligatory NK cell-PSC contact requirement to reciprocally modulate cellular phenotype and function as well as NK cell-mediated cancer cell cytotoxicity (Figure 1D, Supplementary Figure S1F).

Abbreviations: AM, acetyoxymethyl; aPSC, activated pancreatic stellate cell; ATRA, all-trans retinoic acid; CAF, cancer associated fibroblast; CXCL, C-X-C chemokine ligand; ECM, extracellular matrix; hTERT, telomerase reverse transcriptase; MFI, mean fluorescence intensity; NK, natural killer; PDAC, pancreatic ductal adenocarcinoma; PSC, pancreatic stellate cell; qPSC, quiescent pancreatic stellate cell; RAR, retinoic acid receptor; SASP, senescence-associated secretory phenotype; STARPAC, stromal targeting for pancreatic cancer; TME, tumour microenvironment.

This is an open access article under the terms of the [Creative Commons Attribution-NonCommercial-NoDerivs](https://creativecommons.org/licenses/by-nc-nd/4.0/) License, which permits use and distribution in any medium, provided the original work is properly cited, the use is non-commercial and no modifications or adaptations are made.

© 2024 The Author(s). *Cancer Communications* published by John Wiley & Sons Australia, Ltd. on behalf of Sun Yat-sen University Cancer Center.

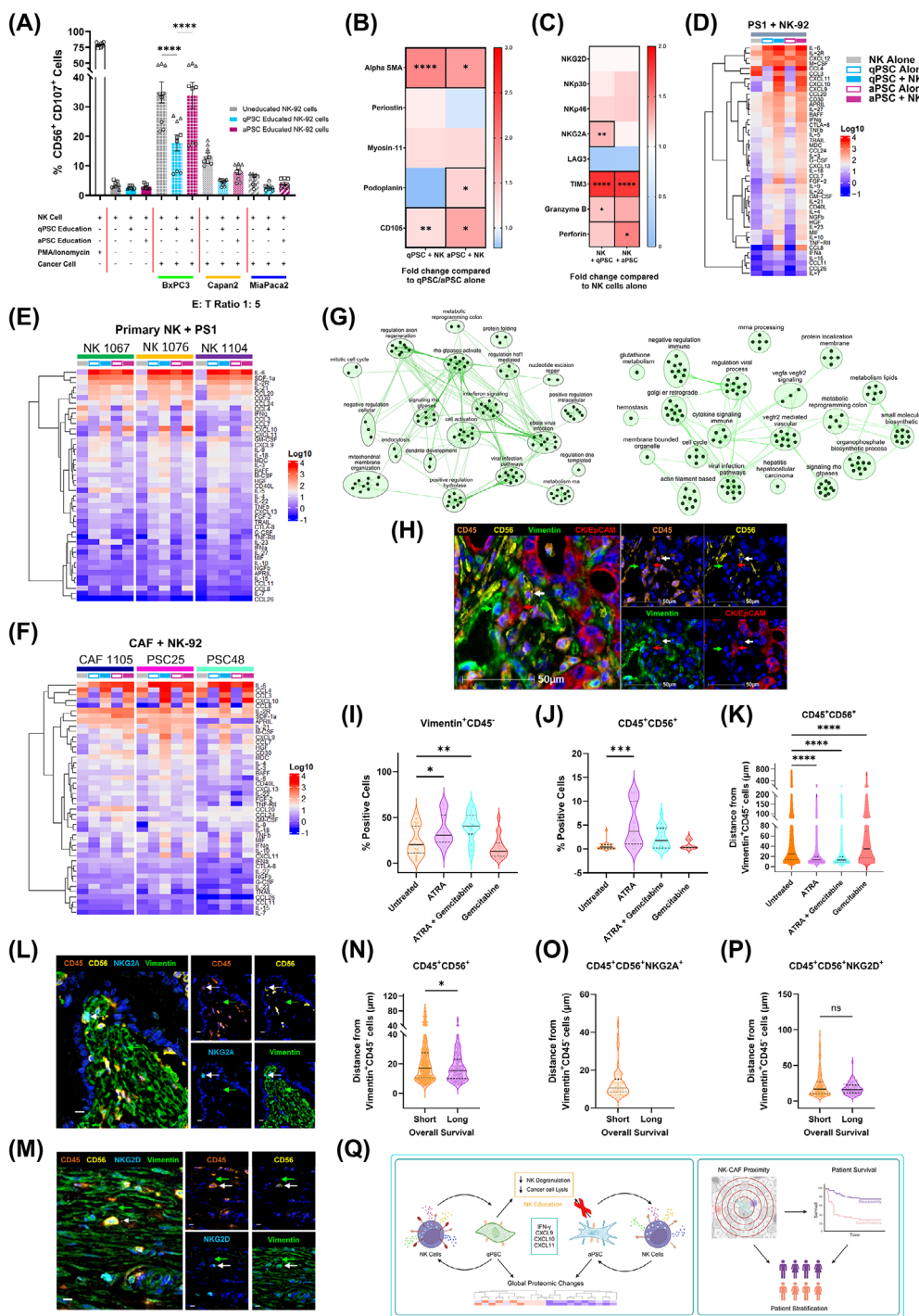


FIGURE 1 NK cells and PSC/CAF exhibit a bidirectional interaction which may have prognostic significance in PDAC. (A) NK-92 cytotoxicity was assessed using a flow cytometry-based degranulation assay. Educated (24h culture with qPSC/aPSC) or uneducated NK-92 cells were incubated with pancreatic cancer cell lines (BxPC3, MiaPaca2, Capan2) for 6h, E: T 1: 5 and NK-92 degranulation assessed via CD107a/b expression. Samples were further stained for the lineage markers CD45 and CD56 before acquisition on the Cytek Aurora (Cytek Biosciences, Fremont, CA). Data were analysed using FlowJo (10.8.1) (BD Biosciences) software and are presented as the percentage of CD107a/b positive NK-92 cells. One-Way ANOVA with Sidak's post-hoc analysis (BxPC3: Uneducated NK-92 vs qPSC educated NK, $P < 0.001$; qPSC educated NK-92 vs aPSC educated NK-92, $P < 0.001$). We determined that qPSC educated NK-92 cells exhibited significantly reduced degranulation in the presence of BxPC3 target cells than did uneducated or aPSC educated cells. Similar trends were observed for all other cancer cell lines. This finding suggests a modulatory role for qPSCs on NK-92 cell function. (B-C) Phenotypic changes in NK-92, qPSC and aPSC following 24h co-culture at a 1: 1 ratio were assessed via spectral flow cytometry. Cells were stained for both surface and intracellular markers to assess phenotypic modulation before acquiring the samples on the Cytek Aurora (Cytek Biosciences, Fremont, CA). Data were analysed using FlowJo (10.8.1) (BD Biosciences) software and are represented as fold change in geometric mean fluorescence intensity (MFI). (B) Fold change in geometric MFI of PSC phenotypic markers in qPSC/aPSCs cultured with NK cells compared to qPSC/aPSC cultured alone.

Data were analysed using One Way ANOVA test with Sidak's post-hoc analysis. (alpha SMA (qPSC alone vs qPSC + NK-92, $P < 0.001$; aPSC alone vs aPSC + NK-92, $P = 0.037$), CD105 (qPSC alone vs qPSC + NK-92, $P = 0.005$; aPSC alone vs aPSC + NK-92, $P = 0.012$), Periostin, Myosin-11, and Podoplanin (aPSC alone vs aPSC + NK-92, $P = 0.037$). (C) Fold change in geometric MFI of phenotypic markers on/in NK-92 cells co-cultured with qPSCs or aPSCs vs NK-92 cells alone. Data were analysed using One-Way ANOVA with Sidak's multiple comparisons (all markers except perforin), or Kruskal-Wallis analysis with Dunn's post hoc (perforin) (NK-92 alone vs NK-92 + qPSC: NKG2A, $P = 0.001$; TIM3, $P < 0.001$; Granzyme B, $P = 0.026$; NK-92 alone vs NK-92 + aPSC: TIM3, $P < 0.001$, Perforin, $P = 0.045$). We identified significant phenotypic alterations in qPSC, aPSC and NK-92 cells in response to direct co-culture suggesting that NK-92 and qPSC/aPSC reciprocally modulate cellular phenotype and function in a bidirectional manner. (D-F) Cellular secretome analysis was carried out by Luminex ELISA following 24h direct co-culture of qPSC/aPSC with NK-92 cells, primary NK cells with qPSC/aPSC or primary CAFs (quiescent/activated with NK-92 cells). Cells were cultured at a 1:1 ratio. Data are presented as the relative cytokine/chemokine abundance (Log10 + 0.1 transformed) in (D) NK-92 cells and qPSC/aPSC cultured alone or in direct contact, (E) primary NK cells derived from PDAC patients alone or in direct culture with PS1 cells, (F) patient derived cancer associated fibroblasts (quiescent/activated) alone or in direct culture with NK-92 cells (abundant: red, lesser abundance: blue). We demonstrated significant secretome changes in response to direct co-culture, with a significant upregulation of interferon- γ and related chemokines observed, suggesting that this pathway may play a key role in the functional and phenotypic changes presented in Figure 1A-C. (G) Mass-spectrometry was used to determine global proteomic changes in NK, qPSC and aPSC cultured in direct co-culture for 24h (1:1 ratio). Data were acquired using the Fourier Transform (FT) and Ion trap (IT) method. Significantly upregulated proteins were subjected to pathway analysis using Metascape and plotted using Cytoscape (version 3.10.1) software. Pathway maps of biological processes upregulated in NK-92 cells cultured with aPSCs vs those cultured with qPSCs and in aPSCs cultured with NK-92 cells vs qPSCs cultured with NK-92 cells are shown in the left and right panels, respectively. These findings demonstrated significant bi-directional interaction between NK and qPSC/aPSC at the proteomic level and further supported involvement of the interferon- γ signalling pathway as a regulator of the phenotypic/functional changes observed. (H-K) The gold standard Pdx1-Cre, LSL-Kras^{+/G12D}, LSL-Trp53^{R172H/+} (KPC) murine model of PDAC was used to assess NK – CAF interaction in vivo. Mice were treated with ATRA, ATRA + Gemcitabine or Gemcitabine alone as previously described [9]. Untreated mice served as the control. When the designated endpoints were reached, tumours were harvested and embedded in paraffin. Whole slide tissue sections were prepared (4 μ m thick) and stained using multiplex immunohistochemistry for CD45, CD56, Vimentin and Cytokeratin/EpCAM. Stained tissue sections were imaged using the Zeiss Axioscan 7 (Zeiss, Oberkochen, Germany) and analysed using HALO software (Indica Labs, Albuquerque, NM, USA). For infiltration analysis, positive cells were scored using the HighPlex FL algorithm package (Indica Labs, Albuquerque, NM, USA). Spatial analysis was conducted using HALO's spatial analysis module (Indica Labs, Albuquerque, NM, USA). (H) Representative image of CD45⁺CD56⁺, Vimentin⁺CD45⁻ and CK/EpCAM⁺Vimentin⁻CD45⁻ cells in tissue from KPC mice. Green arrows indicate Vimentin⁺CD45⁻ cells; White arrows indicate CD45⁺CD56⁺ cells; Red arrows indicate CK/EpCAM⁺Vimentin⁻CD45⁻ cells. (I) Percentage of Vimentin⁺CD45⁻ cells in untreated, ATRA, ATRA + Gemcitabine, or Gemcitabine treated mice. Data were analysed using Kruskal-Wallis analysis with Dunn's post hoc tests (Untreated vs ATRA $P = 0.044$; untreated vs ATRA + Gemcitabine $P = 0.007$). (J) CD45⁺CD56⁺ infiltration in untreated, ATRA, ATRA + Gemcitabine, or Gemcitabine treated mice. Data were analysed using Kruskal-Wallis analysis with Dunn's post hoc tests (Untreated vs ATRA $P < 0.001$). Each data point represents a region of interest analysed. Individual mice are depicted through symbol shape (I, J). (K) Proximity analysis of CD45⁺CD56⁺ to Vimentin⁺CD45⁻ cells in untreated, ATRA, ATRA + Gemcitabine, or Gemcitabine treated mice Data were analysed using Kruskal-Wallis analysis with Dunn's post hoc tests (all post hoc comparisons; $P < 0.001$). Regions of interest: Untreated $n = 20$; ATRA $n = 20$; ATRA + Gemcitabine $n = 20$; Gemcitabine alone $n = 20$; 10 ROIs were selected per mouse. Mice: Untreated $n = 2$; ATRA $n = 2$; ATRA + Gemcitabine $n = 2$; Gemcitabine alone $n = 2$). We identified a significant increase in the number of Vimentin⁺CD45⁻ cells and NK cell infiltrate in response to ATRA treatment. Furthermore, proximity analysis revealed closer proximity between NK cells and CAFs in ATRA treated mice. Taken together these results suggested that ATRA induced modulation of PSC/CAF affects NK cell infiltrate and proximity. (L-P) Multiplex immunohistochemistry of tissue microarray sections was used to assess NK cell infiltrate and CAF expression in PDAC patient samples. Sections were stained using the Leica Bond MAX autostainer (Leica Biosystems Melbourne Pty Ltd, Mt. Waverley, VIC, Australia) and imaged using the Vectra imaging system (Akoya Biosciences, USA). Patient samples were analysed using HALO software (Indica Labs, Albuquerque, NM, USA). For infiltration analysis, positive cells were scored using the HighPlex FL algorithm package (Indica Labs, Albuquerque, NM, USA). Spatial analysis was conducted using HALO's spatial analysis module (Indica Labs, Albuquerque, NM, USA). For the comparison of short and long survivors, patients were dichotomised at a survival interval of 30 months. Statistical analysis was conducted using GraphPad Prism v 9.3 (GraphPad Software, Dotmatics). (L, M) Representative images of CD45⁺CD56⁺NKG2A⁺ (L) and CD45⁺CD56⁺NKG2D⁺ (M) cells in PDAC. Green arrows indicate Vimentin⁺CD45⁻ cells; White arrows indicate CD45⁺CD56⁺NKG2D⁺/CD45⁺CD56⁺NKG2A⁺ cells. (N-P) Violin plots showing results of proximity analysis between CD45⁺CD56⁺ ($P = 0.029$) (N), CD45⁺CD56⁺NKG2A⁺ (O) and CD45⁺CD56⁺NKG2D⁺ (P) cells with Vimentin⁺CD45⁻ cells in short ($n = 48$) and long ($n = 16$) survivors. Data were analysed using Mann-Whitney U-tests. We demonstrated no significant differences in total NK cell infiltrate between short and long survivors, whilst CD45⁺CD56⁺NKG2A⁺ cells were found to be absent in long survivors. Notably, NK cell - CAFs proximity was found to be significantly reduced in long survivors, suggesting that cellular proximity and not total cell infiltrate may play a prognostic role in PDAC. (Q) Summary cartoon of the bidirectional interactions identified in this study (created with BioRender.com). Abbreviations: ANOVA, analysis of variance; aPSC, activated pancreatic stellate cell; ATRA, all-trans retinoic acid; CAF, cancer associated fibroblast; MFI, mean fluorescence intensity; NK, natural killer; PDAC, pancreatic ductal adenocarcinoma; qPSC, quiescent pancreatic stellate cell.

This preliminary cell line work could be confirmed in multiple, independent, primary, PDAC-patient-derived NK cells and CAFs grown from tissues of patients with PDAC (Figure 1E-F). In fact, these functional and phenotypic changes were manifest due to involvement of multiple intra-cellular pathways such as protein folding, interferon and cytokine signalling, chromatin remodelling and nucleotide biosynthesis, as demonstrated by proteomic analysis from cell lysates after direct co-culture (Figure 1G, Supplementary Figure S1G-H). Thus, we demonstrated, a convincing *in vitro* bidirectional, global PSC-NK interaction affecting cancer cell cytotoxicity using cell lines and primary patient derived material; where ATRA was used to modulate PSC, but not NK or cancer cells.

We confirmed these bidirectional interactions in an *in vivo* murine autochthonous, transgenic model of PDAC (Figure 1H) [9], which had been treated with cancer targeting chemotherapy (Gemcitabine) and/or stromal modulating agent (ATRA), compared to vehicle treated animals [9]. We demonstrated stromal modulation with ATRA which resulted in increased Vimentin⁺CD45⁻ cellular density (Figure 1I). Surprisingly, even with just one week's treatment, we saw an increase in overall NK cell infiltrate (CD45⁺CD56⁺) upon stromal modulation with ATRA (Figure 1J). Further, cellular proximity analysis determined that upon stromal modulation (ATRA), CD45⁺CD56⁺ NK cells were significantly closer to Vimentin⁺CD45⁻ CAFs when compared to those animals treated with vehicle control (Figure 1K), confirming that ATRA mediated PSC modulation changes NK cell proximity and infiltrate. Recent independent work complemented our findings by demonstrating that the activation of the retinoic acid receptor (RAR) induced a tumour-suppressive senescence-associated secretory phenotype (SASP) in cancer cells, which can lead to a robust anti-tumour immune response. Thus, combination of RAR activation and chemotherapy enhanced NK-cell-mediated tumour clearance as well as NK cell recruitment to the tumour [10].

Whilst cognate cell surface NK cell receptors are difficult to explore in murine tissues, we demonstrated the importance of cellular proximity in NK: PSC (CAF) interaction in human samples, to further validate this finding. We utilised multiplex immunohistochemistry to explore total NK populations as well as subsets expressing specific activating/inhibitory receptors and their relationship to CAFs (pan-CAF marker vimentin [8]) in human PDAC samples. To investigate the prognostic importance of NK cell infiltrate in PDAC, we dichotomised patients into short (< 30 months, $n = 48$) or long (> 30 months, $n = 16$) survivors, with both groups expressing similar tumour variables known to have a prognostic implication (Supplementary Figure S2). We confirmed the well documented intra- and

inter-tumoral heterogeneity among CAF subtype distribution (Supplementary Figure S3A-B) as well as identified wide NK cell phenotypic heterogeneity (Figure 1L-M, Supplementary Figure S3C-D). Interestingly, no difference was identified in total NK cell infiltrate between short and long survivors (Supplementary Figure S3E). However, CD45⁺CD56⁺NKG2A⁺ cells (but not other subsets) were found to be absent in long survivors (Supplementary Figure S3F-I).

Next, we assessed the role of NK-CAF proximity in PDAC. Using HALO's Spatial Analysis module (Indica Labs) we identified CD45⁺CD56⁺ (NKG2D⁺/NKG2A⁺/NKp46⁺/LAG3⁺) cells within PDAC tissues and assessed their absolute distance to Vimentin⁺CD45⁻ CAFs (Figure 1N-P, Supplementary Figure S3J-K). Long survivors demonstrated shorter spatial distance between CD45⁺CD56⁺ NK cells and CAFs than did short survivors, suggesting that it is the NK cell proximity to CAFs, and not the global NK infiltrate, which impacts patient prognosis (Figure 1N). Notably, activation/quiescence of CAFs in human samples could not be evaluated due to lack of reliable markers to assess these phenotypic states; however, this would be valuable area for further investigation. Taken together, these results suggested that NK interaction with PSC/CAF in PDAC may play a prognostic role and consequently may be used for patient stratification.

In conclusion, this study suggested a bidirectional relationship between NK cells and PSCs in PDAC. We offer novel observational insights into the cell-cell interactions at the phenotypic, functional, and proteomic levels. Additionally, we demonstrated prognostic implications of NK-CAF proximity in PDAC and suggested its potential use as a marker for patient stratification (Figure 1Q). Further work is needed to fully evaluate the mechanistic underpinnings of this dynamic relationship, as well as the up/down regulation of specific NK cell and CAF markers. This may perhaps be achieved through genetically engineered mouse models with modified NK or CAF populations as well as spatial transcriptomics, facilitating a deeper understanding of the long-term sequelae of this dynamic interaction; thus, uncovering potential targets to exploit for the treatment of PDAC.

AUTHOR CONTRIBUTIONS

Design of work: Rachel Elizabeth Ann Fincham, Parthiban Periasamy, Joe Poh Sheng Yeong, and Hemant Mahendrakumar Kocher. Acquisition and analysis: Rachel Elizabeth Ann Fincham, Parthiban Periasamy, Craig Ryan Joseph, Jia Meng, Jeffrey Chun Tatt Lim, Felicia Wee, Jiangfeng Ye, Li Yen Chong, Joe Poh Sheng Yeong, and Hemant Mahendrakumar Kocher. Methodological troubleshooting: Rachel Elizabeth Ann Fincham, Parthiban

Periasamy, Craig Ryan Joseph, Jia Meng, Jeffrey Chun Tatt Lim, Felicia Wee, Konstantinos Stasinou, Michelle Rodrigues Goulart, Joe Poh Sheng Yeong, and Hemant Mahendrakumar Kocher. Interpretation: Rachel Elizabeth Ann Fincham, Parthiban Periasamy, Joe Poh Sheng Yeong, and Hemant Mahendrakumar Kocher. Writing: Rachel Elizabeth Ann Fincham, Denise Goh, Parthiban Periasamy, Joe Poh Sheng Yeong, Hemant Mahendrakumar Kocher, and Bijin Veonice Au. All authors read and approved the final manuscript.

ACKNOWLEDGMENTS

We thank members of the Kocher (Centre for Tumour Biology, Barts Cancer Institute-a Cancer Research United Kingdom [CRUK] Centre of Excellence, Queen Mary University of London, London, UK) and Yeong (Institute of Molecular and Cell Biology [IMCB], Agency of Science, Technology and Research [A*STAR], Singapore) laboratories for critical appraisal and suggestions throughout this project. We thank Radoslaw Sobota (Functional Proteomics Laboratory, Institute of Molecular and Cell Biology [IMCB], Agency of Science, Technology and Research [A*STAR], Singapore) for his support with mass spectrometry sample acquisition.

CONFLICT OF INTEREST STATEMENT

The authors declare that no conflict of interest exists.

FUNDING INFORMATION

This research is partly supported by Barts Charity and A*STAR Research Attachment Programme (ARAP) PhD studentship. Pancreatic Cancer Research Fund Tissue Bank is funded by Pancreatic Cancer Research Fund. Hemant Kocher is supported by NIHR Barts Biomedical Research Centre. Barts Cancer Institute is supported by Cancer Research UK.

DATA AVAILABILITY STATEMENT

Data is available from the corresponding author on reasonable request.

ETHICS APPROVAL AND CONSENT TO PARTICIPATE

Ethics approval for the use of human pancreatic cancer tissue was obtained from City and East London Research Ethics Committee (REC0029 07/0705/87). Each participant signed an informed consent before participating to this study. Primary cells were provided by Pancreatic Cancer Research Fund Tissue Bank.

Rachel Elizabeth Ann Fincham^{1,2} 
Parthiban Periasamy² 

Craig Ryan Joseph² 

Jia Meng² 

Jeffrey Chun Tatt Lim² 

Felicia Wee² 

Konstantinos Stasinou¹ 

Michelle Rodrigues Goulart¹ 

Jiangfeng Ye² 

Li Yen Chong² 

Bijin Veonice Au² 

Denise Goh² 

Joe Poh Sheng Yeong^{2,3,4,5} 

Hemant Mahendrakumar Kocher^{1,6} 

¹Centre for Tumour Biology, Barts Cancer Institute-a Cancer Research United Kingdom (CRUK) Centre of Excellence, Queen Mary University of London, London, UK

²Institute of Molecular and Cell Biology (IMCB), Agency of Science, Technology and Research (A*STAR), Singapore, Singapore

³Centre for Quantitative Medicine, Duke-National University of Singapore (NUS) Medical School, Singapore, Singapore

⁴Department of Anatomical Pathology, Singapore General Hospital, Singapore, Singapore

⁵Cancer Science Institute of Singapore, National University of Singapore, Singapore, Singapore

⁶Barts and the London Hepato-Pancreato-Biliary (HPB) Centre, The Royal London Hospital, Barts Health National Health Service Trust, London, UK

Correspondence

Hemant Mahendrakumar Kocher, Queen Mary University of London, Centre for Tumour Biology, Barts Cancer Institute-a Cancer Research United Kingdom (CRUK) Centre of Excellence, Charterhouse Square, London EC1M 6BQ, United Kingdom.
Email: h.kocher@qmul.ac.uk

Joe Poh Sheng Yeong, Institute of Molecular and Cell Biology (IMCB), 61 Biopolis Drive, Proteos, Singapore 138673.

Email: yeongps@imcb.a-star.edu.sg

ORCID

Rachel Elizabeth Ann Fincham  <https://orcid.org/0000-0002-4699-5002>

Parthiban Periasamy  <https://orcid.org/0000-0003-3709-8008>

Craig Ryan Joseph  <https://orcid.org/0009-0004-5326-9692>

Jia Meng  <https://orcid.org/0000-0003-1019-8885>

Jeffrey Chun Tatt Lim  <https://orcid.org/0000-0002-8903-8843>

Felicia Wee  <https://orcid.org/0009-0004-7624-3751>

Konstantinos Stasinou  <https://orcid.org/0000-0001-5334-3267>

Michelle Rodrigues Goulart  <https://orcid.org/0000-0001-8333-3908>

Jiangfeng Ye  <https://orcid.org/0000-0001-6963-2450>

Li Yen Chong  <https://orcid.org/0000-0002-4623-4633>

Denise Goh  <https://orcid.org/0000-0003-4598-4181>

Joe Poh Sheng Yeong  <https://orcid.org/0000-0002-6674-7153>

Hemant Mahendrakumar Kocher  <https://orcid.org/0000-0001-6771-1905>

REFERENCES

- Rahib L, Wehner MR, Matrisian LM, Nead KT. Estimated Projection of US Cancer Incidence and Death to 2040. *JAMA Netw Open*. 2021;4(4):e214708.
- Froeling FE, Feig C, Chelala C, Dobson R, Mein CE, Tuveson DA, et al. Retinoic acid-induced pancreatic stellate cell quiescence reduces paracrine Wnt- β -catenin signaling to slow tumor progression. *Gastroenterology*. 2011;141(4):1486-97, 97.e1-14.
- Neuzillet C, Tijeras-Raballand A, Ragulan C, Cros J, Patil Y, Martinet M, et al. Inter- and intra-tumoural heterogeneity in cancer-associated fibroblasts of human pancreatic ductal adenocarcinoma. *J Pathol*. 2019;248(1):51-65.
- Kocher HM, Basu B, Froeling FEM, Sarker D, Slater S, Carlin D, et al. Phase I clinical trial repurposing all-trans retinoic acid as a stromal targeting agent for pancreatic cancer. *Nature Communications*. 2020;11(1):4841.
- Delvecchio FR, Fincham REA, Spear S, Clear A, Roy-Luzarraga M, Balkwill FR, et al. Pancreatic Cancer Chemotherapy Is Potentiated by Induction of Tertiary Lymphoid Structures in Mice. *Cell Mol Gastroenterol Hepatol*. 2021;12(5):1543-65.
- Aguirre GA, Goulart MR, Dalli J, Kocher HM. Arachidonate 15-lipoxygenase-mediated production of Resolvin D5(n-3 DPA) abrogates pancreatic stellate cell-induced cancer cell invasion. *Front Immunol*. 2023;14:1248547.
- Goulart MR, Watt J, Siddiqui I, Lawlor RT, Imrali A, Hughes C, et al. Pentraxin 3 is a stromally-derived biomarker for detection of pancreatic ductal adenocarcinoma. *npj Precision Oncology*. 2021;5(1):61.
- Hutton C, Heider F, Blanco-Gomez A, Banyard A, Kononov A, Zhang X, et al. Single-cell analysis defines a pancreatic fibroblast lineage that supports anti-tumor immunity. *Cancer Cell*. 2021;39(9):1227-44.e20.
- Carapuca EF, Gemenetzidis E, Feig C, Bapiro TE, Williams MD, Wilson AS, et al. Anti-stromal treatment together with chemotherapy targets multiple signalling pathways in pancreatic adenocarcinoma. *J Pathol*. 2016;239(3):286-96.
- Colucci M, Zumerle S, Bressan S, Gianfanti F, Troiani M, Valdata A, et al. Retinoic acid receptor activation reprograms senescence response and enhances anti-tumor activity of natural killer cells. *Cancer Cell*. 2024;42(4):646-61.e9.

SUPPORTING INFORMATION

Additional supporting information can be found online in the Supporting Information section at the end of this article.